# Microelectromechanical resonators based on an all polymer/carbon nanotube composite structural material

P. M. Sousa,[1] M. Gutiérrez,[2] E. Mendoza,[3] A. Llobera,[2] V. Chu,[1] and J. P. Conde[1,4,a)]
[1]*INESC Microsistemas e Nanotecnologias (INESC MN) and IN-Institute of Nanoscience and Nanotechnology, Rua Alves Redol, 9, 1000-029 Lisboa, Portugal*
[2]*Instituto de Microelectronica de Barcelona (IMB-CNM, CSIC), Barcelona, Spain*
[3]*Grup de Nanomaterials Aplicats, Centre de Recerca en Nanoenginyeria, Universitat Politècnica de Catalunya, c/Pascual i Vila 15, 08028, Barcelona, Spain*
[4]*Department of Bioengineering, Instituto Superior Técnico, 1000-049 Lisbon, Portugal*

(Received 6 June 2011; accepted 12 July 2011; published online 29 July 2011)

Carboxylated multi-wall carbon-nanotubes (CNTs) monolayers are integrated on microfabricated all-polymer micro-electromechanical systems (pMEMS) resonator bridges on glass substrates. The structural layer of the MEMS bridges is a multilayer blended conductive polymer based on poly(3,4-ethylenedioxythiophene):poly(styrenesulfonate) (PEDOT:PSS) to which functionalized CNT monolayers are electrostatically attached. The resonance frequency ($f_{res}$) of electrostatically actuated pMEMS bridges was measured as a function of their length (32–67 $\mu$m) for different multilayer compositions. A significant increase in $f_{res}$ and quality factor ($Q$) with the addition of CNT monolayers to the PEDOT:PSS structural material is observed, demonstrating that CNT monolayers can be used to modulate pMEMS resonator properties. © *2011 American Institute of Physics*. [doi:10.1063/1.3621861]

Micro-electromechanical systems (MEMS) are three-dimensional microdevices that can act as sensors, actuators, or passive structures. Most commercial products based on MEMS currently use single-crystal silicon or polycrystalline silicon as the structural material. However, due to their relatively low cost, simple processing, and variety of chemical structures available, polymer based MEMS (pMEMS) is an expanding research field.[1,2] The potential to engineer the mechanical, electronic, and chemical properties of pMEMS over a wide range is an advantage over conventional silicon MEMS. Polymers have low density, low Young's modulus ($E$), and high yield strength. The bulk mechanical and also the surface properties of polymers (as well as their blends and/or multilayers) can be adjusted by changing chemical and physical parameters and may lead to the development of novel sensors. An obvious application of pMEMS is in the "flexible and stretchable electronics" field in which polymers can work not only as the substrate but also as electronic or micromechanical functional devices.

Different types of all-polymer MEMS actuators have been demonstrated such as, polydimethylsiloxane (PDMS) cantilevers,[3,4] SU-8 microgrippers, accelerometers and variable optical attenuators,[5,6] freely suspended microstructures, and vertical comb actuators based on poly(methyl methacrylate) (PMMA) and polystyrene.[7,8] To achieve electrostatic actuation of a MEMS structure, a conductive structural material or layer is needed. In this work, we report the demonstration of an all-polymer electrostatically actuated MEMS resonator based on the conductive polymer, poly(3,4-ethylenedioxythiophene): poly(styrenesulfonate) (PEDOT:PSS) blend as the structural material[9] whose mechanical and resonance properties have been modified by the integration of carbon nanotubes (CNTs).

Microbridges were processed on glass substrates by surface micromachining. Those structures showed a high sensitivity to the applied electrical force, and a quality factor ($Q$) in vacuum of the order of 100. CNTs, besides their high aspect ratio and exceptional electrical and thermal properties, have been shown to have very high axial $E \sim 1$ TPa.[10] Hence, in this work, CNTs are investigated as an ideal reinforcement phase for creating electrically conductive polymer-CNT composites for integration in pMEMS. Important challenges to address are the dispersion of CNTs oriented uniaxially in the host polymer matrix (thus maximizing the composite stiffness) and overcoming the CNTs strong tendency to agglomerate.[11]

A multilayer consisting of spin coated PEDOT:PSS interspersed with carboxylated multi-wall CNT monolayers was developed to function as the structural layer in pMEMS microresonators. The conductive PEDOT:PSS mixture was prepared with the following composition in %(v/v): isopropanol (7.6%), PMMA (photoresist AR-P679.04 - 950k) (1.5%) and its solvent 2-methoxy-1-methylethyl acetate (PGMA, AR300-12) (7.6%). The PEDOT:PSS thin film was prepared by spin-coating and, after baking at 100 °C for 2 h, was $NH_2$-functionalized with 3-aminopropyltriethoxy silane (APTES) 10% (v/v) in $H_2O$. The carboxylated CNTs (NC 3101, average diameter and length of 9.5 nm and 1.5 $\mu$m, respectively, in a phosphate buffer solution (100 $\mu$g/ml)) were electrostatically attached by dip coating (overnight) to the functionalized surface through the interaction between the positively charged amine groups and the negatively charged carboxyl groups. A randomly oriented CNT monolayer was obtained as shown in the micrograph of Fig. 1(a) and with a surface roughness of 20–30 nm as determined from the atomic force microscopy (AFM) analysis [Fig. 1(b)]. Finally, a protective 100 nm layer of PMMA was spin coated (PEDOT:PSS/CNT/PMMA ≡ CNT1) on top. For comparison, a structure using a single PEDOT:PSS/PMMA

a)Author to whom correspondence should be addressed. Electronic mail: joao.conde@ist.utl.pt.

 

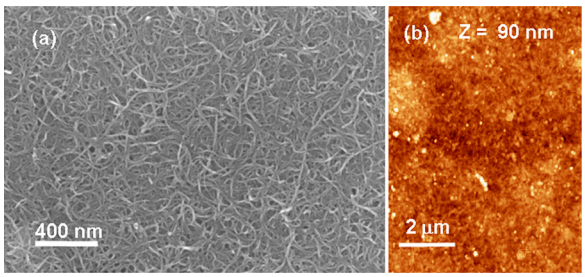


FIG. 1. (Color online) (a) Scanning electron microscope (SEM) and (b) AFM micrographs of a monolayer of carboxylated multi-wall carbon nanotubes attached to an APTES-functionalized PEDOT:PSS thin film.

(≡PEDOT) layer and a structure using a double layer (PEDOT:PSS/CNT) × 2/PMMA structure (≡CNT2) were also micro-fabricated and characterized. For CNT2 the 1st PEDOT:PSS layer is 300 nm thick and the 2nd PEDOT:PSS layer is 100 nm thick. All fabricated structures have a total thickness ($t$) of ~500 nm (~400 nm of overall thickness of the PEDOT:PSS layers and a 100 nm PMMA protective layer on the top). The micro fabrication process, which was carried out at $T \leq 110\,^{\circ}\mathrm{C}$ is schematically described in Fig. 2. TiW (200 nm) is deposited using radio-frequency (RF) magnetron sputtering and is patterned by wet etching as the bottom contacts to the bridge and gate. Aluminium is deposited by RF magnetron sputtering and patterned by wet etching to form the sacrificial layer (1.3 $\mu$m thick). The polymer structural layers are spin coated at room temperature (after each spin coat the film is baked at 100 °C for 1 min), and the stack is patterned by plasma etching using an Al hard mask. A $FeCl_3 \cdot 6H_2O$ solution (0.05 g/ml) is used as the sacrificial layer etchant. As-spun PEDOT:PSS thin films have an electrical conductivity ($\sigma$) of ~1 S/cm. However, processing degrades $\sigma$ significantly. Microfabricated PEDOT:PSS bridges have $\sigma = 5 \times 10^{-5}$ S/cm, but their conductivity increases with the presence of CNT layers (CNT1: $\sigma = 9 \times 10^{-4}$ S/cm; CNT2: $\sigma = 4 \times 10^{-3}$ S/cm). Microbridges with widths ($w$) of 10 $\mu$m and lengths ($L$) from 32 to

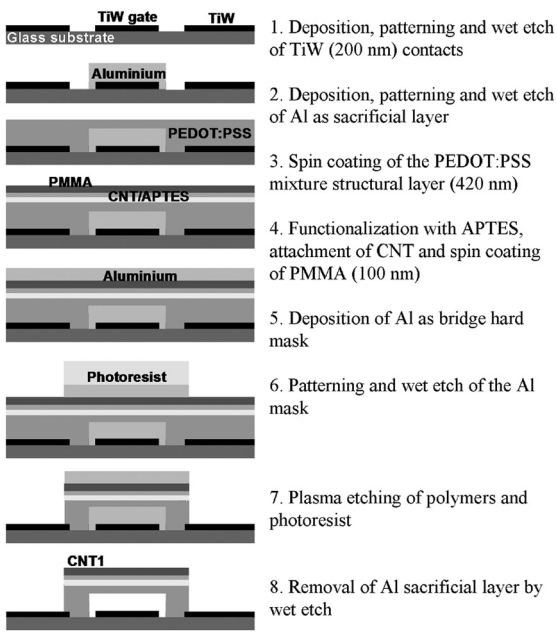


FIG. 2. Schematic diagram (longitudinal cross section) of the micro-fabrication process of PEDOT:PSS/CNT/PMMA (CNT1) bridges.

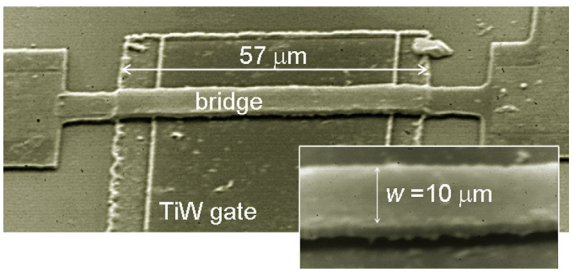


FIG. 3. (Color online) SEM micrograph of a CNT1 bridge with a ~1.3 $\mu$m air gap height ($d$), a length of 57 $\mu$m ($L$), a width of 10 $\mu$m ($w$), and a thickness of 520 nm.

67 $\mu$m were fabricated and characterized electromechanically. An SEM micrograph of a typical bridge structure is shown in Fig. 3. The resonance characteristics (fundamental flexural resonance frequency, $f_{res}$, and $Q$) were measured in vacuum ($10^{-6}$ Torr) at room temperature by applying a voltage with DC and AC components between the bridge and the gate electrodes. An AC voltage of 1.26 V was used in all experiments. The resonance frequency of individual bridges was monitored by using an optical detection setup described in Ref. 12. Representative resonance peaks of PEDOT and CNT2 bridges are shown in Fig. 4. In Fig. 5 $f_{res}$ is plotted as a function of $L$ for the different multilayer bridges.

Fig. 5 shows that the addition of a CNT layer significantly increases $f_{res}$ of the pMEMS resonator. Analytical mechanical modelling of $f_{res}$ for the different multilayer bridges was made using a model described previously.[13] For a clamped-clamped bridge with a given number of layers, the fundamental resonance frequency of the flexural mode is approximately given by

$$f_{res} = \sqrt{12.7\frac{(EI)_{\mathrm{eff}}}{\mu_{\mathrm{eff}}L^4} + 0.6\frac{wt_{\mathrm{eff}}}{\mu_{\mathrm{eff}}L^2}\sigma_0}, \qquad (1)$$

where $(EI)_{\mathrm{eff}}$ is the effective rigidity of the multilayer microbridge (as defined in Ref. 13), $\mu_{\mathrm{eff}}$ is the mass per unit length of the suspended bridge, $t_{\mathrm{eff}}$ is the total thickness, and $\sigma_0$ is the residual axial stress. The 1st term in Eq. (1) represents the contribution of the rigidity of the structure (proportional to $1/L^2$) and the second term the contribution of its residual axial stress ($\sigma_0$) proportional to $1/L$. The experimental results for the PEDOT bridges show that $f_{res}$ follows approximately a $1/L^2$ dependence. However, to obtain a good fit, an axial

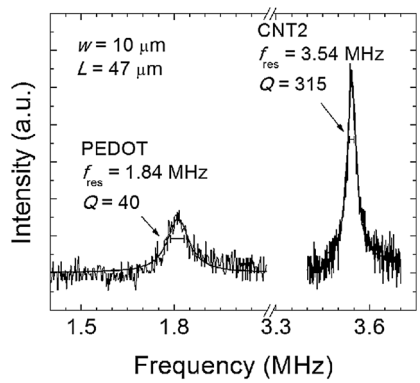


FIG. 4. Characteristic electrostatically actuated and optically detected fundamental flexural resonance peak shapes of PEDOT:PSS/PMMA (PEDOT) and (PEDOT:PSS/CNT) × 2/PMMA (CNT2) bridges.

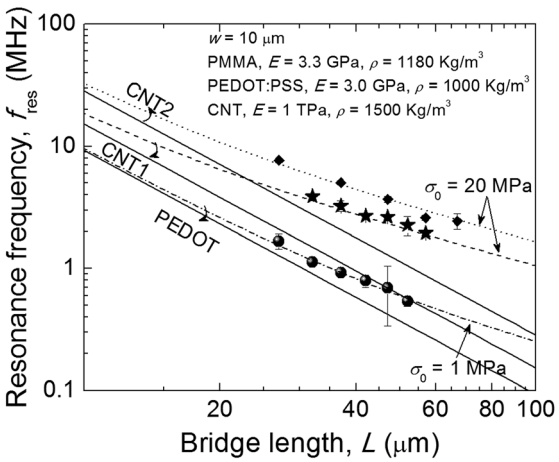


FIG. 5. Flexural resonance $f_{res}$ measured at $10^{-6}$ Torr as a function of $L$ for the pMEMS multilayer structures: PEDOT (•), CNT1 (★) and CNT2 (◆). Solid lines represent simulated $f_{res}$ values considering axial stress-free bridges ($f_{res} \propto 1/L^2$). Dashed lines represent simulated $f_{res}$ values including axial stress, $\sigma_0$, of 1 MPa for PEDOT and 20 MPa for CNT1 and CNT2 bridges.

stress contribution of $\sigma_0 = 1$ MPa is required. The following structural parameters were also used for the fits: $E_{PEDOT:PSS} = 3.0$ GPa, $\rho_{PEDOT:PSS} = 1000$ kg/m$^3$, $t_{PEDOT:PSS} = 420$ nm and $E_{PMMA} = 3.3$ GPa, $\rho_{PMMA} = 1180$ kg/m$^3$, and $t_{PMMA} = 100$ nm$^3$. The CNT monolayer was modeled as a 9.5 nm thick continuous layer (corresponding to the average diameter of the CNT) with an average $\rho_{CNT} = 1500$ kg/m$^3$. A single CNT has an $E \sim 1$ TPa but CNT thin films (also called buckypaper) are predicted to have lower $E$ values. The highest experimental $E$ value found in literature for (single wall) CNT thin films is 357 GPa.[14] For the simulation, effective $E_{CNT}$ values ranging from 1 GPa to 1 TPa were considered. However, the experimental values of $f_{res}$ for the CNT1 and CNT2 bridges show a much stronger $1/L$ component than the PEDOT bridges, and the simulated results were less sensitive to the exact value of $E_{CNT}$ since the dominant contribution to $f_{res}$ is due to the residual stress. Both the experimental results and the simulations suggest that the axial stress present in the CNT-containing multilayers is higher than the CNT-free cases and a value of $\sigma_0 = 20$ MPa for both CNT1 and CNT2 structures was required to obtain a good fit.

In Fig. 6 the $Q$'s obtained for the different structures are shown. For PEDOT bridges $Q$'s $\sim 100$ were obtained. The addition of a CNT layer significantly increases the $Q$-values which approach 1000 for the CNT2 bridges. The most significant source of energy loss (in the form of heat) for polymer microresonators is expected to come from internal friction when the bonds in the polymer structure chains move during the vibration of the structure.[9] The higher stress observed in the multilayer bridges suggests the presence of a strong interfacial adhesion between the CNTs and the polymer matrix.[11] The CNT monolayers are expected to have high thermal conductivity[15] and could help dissipate the heat produced by the internal friction of the polymer and thus lead to the observed increase in $Q$.

All-polymer, electrostatically actuated MEMS resonator bridges based on PEDOT:PSS blended conductive polymer with integrated carboxylated multi-wall CNT monolayers were microfabricated and their electrostatically actuated resonance frequency and quality factor were measured as a function of

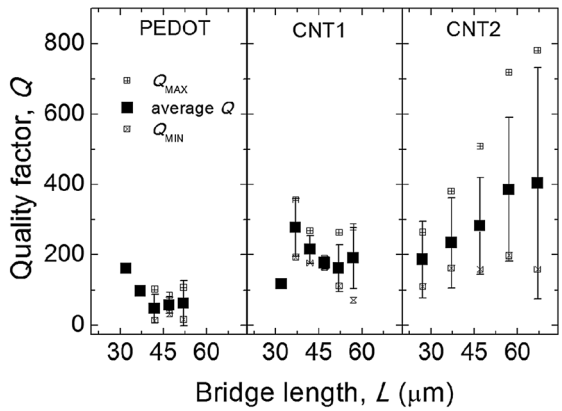


FIG. 6. Mean quality factor, $Q$, as a function of $L$ for polymer bridges with different multilayer structures. The error bars correspond to the standard deviation. Also shown are the maximum and minimum values of $Q$ obtained for a given $L$.

the structure of the bridge and the length of the resonator. The addition of CNT monolayers allowed the tuning of the resonance frequency of the composite and the improvement of the $Q$ of the resonator. The $f_{res}$ for CNT-polymer composite bridges is dominated by the presence of increased axial stress. Molecular control of the CNT interaction with the polymer layers may offer a way to control the axial stress of the polymer structural layer and, consequently, the resonator properties. In this letter, this interaction was achieved via electrostatic interaction, but covalent bonding and hydrophobic interactions can also be designed into the system.

The authors wish to thank J. Bernardo, F. Silva, and V. Soares for their help in cleanroom processing and characterization. This work was supported by financing through the Portugal-Spain Nanotechnology project "Integrated Lab-On-Chip Platforms for Medical Diagnostics," Fundação para a Ciência e a Tecnologia (Portugal) through plurianual financing of the Assoc. Lab. IN and the project NEMS (PTDC/CTM/72772/2006) and the Ministerio de Ciencia e Innovación (Spain) for funding through project EUI2008-00120. P.M.S. also acknowledges FCT for a post-doctoral grant BPD 44425/2008.

[1]S. R. Forrest, Nature (London) **428**, 911 (2004).
[2]C. Liu, Adv. Mater. **19**, 3783 (2007).
[3]A. P. Gerratt, M. Tellers, and S. Bergbreiter, *2011 IEEE 24th International Conference on Micro Electro Mechanical Systems 23–27 January 2011* (IEEE, Cancun, Mexico), pp. 332–335.
[4]A. Llobera, V. J. Cadarso, K. Zinoviev, C. Domínguez, S. Büttgenbach, and J. A. Plaza, IEEE Photonics Technol. Lett. **21**, 79 (2009).
[5]J. Chu, R. Zhang, and Z. Chen, J. Micromech. Microeng. **21**, 054030 (2011).
[6]A. Llobera, V. Seidemann, J. A. Plaza, V. J. Cadarso, and S. Büttgenbach, J. Microelectromech. Syst. **16**, 111 (2007).
[7]N. Ferrell, J. Woodard, and D. Hansford, Biomed. Microdevices **9**, 815 (2007).
[8]S. Amaya, D. V. Dao, and S. Sugiyama, J. Micromech. Microeng. **21**, 065032 (2011).
[9]G. Zhang, V. Chu, and J. P. Conde, J. Appl. Phys. **101**, 064507 (2007).
[10]M.-F. Yu, O. Lourie, M. J. Dyer, K. Moloni, T. F. Kelly, and R. S. Ruoff, Science **287**, 637 (2000).
[11]X. Xu, M. M. Thwe, C. Shearwood, and K. Liao, Appl. Phys. Lett. **81**, 2833 (2002).
[12]J. Gaspar, V. Chu, and J. P. Conde, J.Appl. Phys. **93**, 10018 (2003).
[13]S. B. Patil, V. Chu, and J. P. Conde, J. Micromech. Microeng. **19**, 025018 (2009).
[14]K. Koziol, J. Vilatela, A. Moisala, M. Motta, P. Cunni, M. Sennett, and A. Windle, Science **318**, 1892 (2007).
[15]A. E. Aliev, M. H. Lima, E. M. Silverman, and R. H. Baughman, Nanotechnology **21**, 035709 (2010).